

# A Temporal Bias Correction using a Machine Learning Attention model

Omer Nivron<sup>1</sup> and Damon J. Wischik<sup>2</sup>

<sup>1</sup>University of Cambridge, Department of Computer Science and Technology, Cambridge, UK. [on234@cam.ac.uk](mailto:on234@cam.ac.uk)

<sup>2</sup>University of Cambridge, Department of Computer Science and Technology, Cambridge, UK

**Keywords:** Bias-Correction; Time-series; Heatwaves; Machine-Learning; Attention

## Abstract

Climate models are biased with respect to real world observations and usually need to be calibrated prior to impact studies. The suite of statistical methods that enable such calibrations is called bias correction (BC). However, current BC methods struggle to adjust for temporal biases, because they disregard the dependence between consecutive time-points. As a result, climate statistics with long-range temporal properties, such as heatwave duration and frequency, cannot be corrected accurately, making it more difficult to produce reliable impact studies on such climate statistics. In this paper, we offer a novel BC methodology to correct for temporal biases. This is made possible by i) re-thinking BC as a probability model rather than an algorithmic procedure, and ii) adapting state-of-the-art machine-learning (ML) probabilistic attention models to fit the BC task. With a case study of heatwave duration statistics in Abuja, Nigeria, and Tokyo, Japan, we show striking results compared to current climate model outputs and alternative BC methods.

## Impact Statement

Climate models are biased. Bias Correction (BC) is a suite of statistical methods to address those biases and adjust climate model statistics to enable more precise and localised impact studies. However, to date, no BC can adjust for long-range temporal properties, relevant to infer statistics such as heatwave duration. We offer a novel methodology for temporal BC — this is made possible by adapting state-of-the-art machine-learning (ML) attention models to fit the BC task. We show striking results compared to current climate model outputs and alternative BC methods with a case study of heatwave duration statistics in Abuja, Nigeria, and Tokyo, Japan. The results are relevant to a wide audience, ranging from climate scientists to policy-makers.

## 1. Introduction

Climate models are biased with respect to observations [32, 7, 39], affecting impact studies in domains such as the economy [42, 31, 41], human migration [10], biodiversity [2], hydrology [16, 8, 34] and agronomy [9, 1], subsequently influencing policy-making and public awareness. (see Stainforth et al. [38] for a detailed discussion on reasons for these biases.) Climate scientists have developed a suite of tools termed jointly bias correction (BC) to correct these biases and provide output statistics that more closely match when compared to past observations. Most BC methods are univariate, correcting for a single one-dimensional physical variable in a single location (e.g., the summer daily mean air temperatures in London [20]). The most popular univariate methods are: mean correction [49] (also

called “Delta” methods), variance correction [3, 20, 30, 18, 22, 13, 37] and empirical quantile mapping (EQM) and its variants [20, 25, 36, 48, 17, 40, 43, 12, 47, 23]. These univariate methods, as Vrac et al. [46] explain, cannot correct biases relating to temporal dependencies in the climate model simulations and that if corrected, the biases will propagate to impact studies [4]; they cannot correct for temporal dependencies since they throw away temporal information. Some multivariate BC approaches have been developed to correct properties of multidimensional distributions [35, 33, 6, 11, 45]. However, none of these BC methods is designed to correct for statistics that rely on the joint behaviour of consecutive time-points, such as heatwaves, as pointed out by Francois et al. [15] and also by Vrac et al. [46].

To address the gap, we have devised a novel machine learning (ML) methodology based on attention models [29, 44] — our contribution in this paper. As a first step, we have recast the BC method as a probability model. In a second step, we plugged the – now probabilistic BC – into our probabilistic ML attention model. moving from the typical BC task formulation: “how to match the histogram of observations to the histogram of the climate model?” to the formulation – “how to create a corpus of matched pairs of time-series trajectories?” – that can be plugged into different attention models.

To showcase the strength of our methodology, we use the case study of heatwave duration statistics in Abuja, Nigeria and Tokyo, Japan. We use the simplified heatwave duration definition (as a proof of concept): at least three consecutive days above a chosen absolute value in °C. Our results are striking: our model’s RMSE is 26% lower than the second-best model in Tokyo. For this location our model consistently outperforms the alternatives on the heatwave duration statistic. For example, for different heatwave thresholds, our model misestimated between 8.5% to 20% of the observed heatwaves (in the worst-case scenario). In contrast, the second-best BC model misestimation was between 18% to 66% during a 20-year period. In Abuja, our model’s RMSE is 22% lower than the second-best model. Similarly to the results in Tokyo, our model consistently outperforms the alternatives on the heatwave duration statistic. For example, for different heatwave thresholds, our model misestimated between 0% to 26% of the observed heatwaves (in the worst-case scenario). In contrast, the second-best BC model misestimation was between 2% to 31% during a 20-year period.

## 2. Reference and model data

In any BC task we match data from a climate model to real world observations. For the climate model data, we chose the 32 initial condition runs from the climate model of the Institut Pierre-Simon Laplace (IPSL) [26, 5, 21] under the sixth International Coupled Model Intercomparison Project (CMIP6) [14] historical experiment. The data is obtained at a 1-day frequency for the variable ‘tmax’, representing the maximum temperature 2 meters above the surface. The IPSL model is run at a 250km nominal resolution and is not re-gridded. For the case studies, we take the closest geographical point to Abuja, Nigeria, and the closest point to Tokyo, Japan, from 1948-2008.

For the observational data, we use two different Reanalysis tools:

- For Abuja, Nigeria, we use the NCEP-NCAR Reanalysis 1 [24] of the National Oceanic and Atmospheric Administration (NOAA). The data is obtained in six-hourly daily measurements for the variable ‘tmax’, the maximum temperature 2 meters above the surface, and is averaged to daily measurements. The resolution is 2.5 degrees globally in both the north-south and east-west directions and is not regridded. We chose the closest geographical point to Abuja, Nigeria.
- For Tokyo, Japan, we use the ERA5 reanalysis [19] from the European Centre for Medium-Range Weather Forecasts (ECMWF). The data is obtained daily for the variable ‘mx2t’, the maximum temperature 2 meters above the surface. The resolution is 0.25 degrees globally in both the north-south and east-west directions and is not regridded. We chose the closest geographical point to Tokyo, Japan.

We use two different reanalysis tools, NCEP-NCAR and ERA5, to show that the methodology is not limited to one setup. We hypothesize that the model will also work for many different setups of (climate model, reanalysis tool) pairs.

### 3. Methodology

ML attention models are probability models. To use these models for our task, we cast the classic BC – typically treated as an algorithmic procedure – as a probability model. This point becomes possible because all BC procedures – as we will show example of next – are implicit probability models.

#### 3.1. Univariate BC as a probability model

An example demonstrates best the implicit probability nature of BC methods. In the following, we examine the mean shift [49] (used, for example, by Mora et al. [28] for heatwave mortality impacts). In a mean shift, observations and climate model outputs are collected over a reference period and the difference between their means is calculated. The difference is then added to future climate projections, the collection of which is collapsed to a 1-D histogram. The 1-D histogram disregards the time index. As a result, the mean shift, or any classic univariate BC, does not allow us to reconstruct the time series it originated from (see Appendix, Figure 14 for an illustration). This is exactly why we cannot use these methods to correct climate statistics that are time-dependent such as heatwave duration.

The mean shift procedure yields itself to a probabilistic interpretation (angle): let  $Y_t^o, Y_t^g$  be random variables representing the temperatures at time-point  $t$  for observations and climate model respectively (we represent random variables with a capital letter and specific values in lowercase letters). Now the following probability model can be written:

$$y_t^o = y_t^g + c + \epsilon_t$$

where  $\epsilon_t$  is an instance of  $E_t \sim \text{Normal}(0, \sigma^2)$  and  $c$  is a learned parameter. To find  $c$ , we can use standard linear regression packages (standard linear regression uses maximum likelihood as its objective to learn the parameters – full derivation using maximum likelihood showing the equivalence of the procedural approach and the probability model are in the appendix A.) As a trivial extension, the mean and variance shift probability model is:

$$y_t^o = m \times y_t^g + c + \epsilon_t$$

where both  $m, c$  are learned parameters using standard linear regression (again using the maximum likelihood objective).

The probabilistic interpretation of the mean shift provides us with two takeaways: first, we already use probability models (implicit or explicit) in BC. In that case, we can harness the state-of-the-art ML models that are probability models. Second, in contrast to the mean shift, and any other univariate BC, we do not need to aggregate or collapse our raw data before employing our BC, because the the subscript  $t$  in a probabilistic model can indicate a generic time-point — i.e., it is valid for time-points on any chosen granularity, from hourly to daily to yearly.

From the probabilistic model perspective of the mean shift (or mean and variance shift), it is clear that we cannot use it to correct time-dependent statistics since the random variables  $Y_{t_i}^o, Y_{t_j}^o$  are independent of each other for any  $i \neq j$  — equivalent to throwing away all temporal correlation information.

#### 3.2. Proposed probability model

Differently from the univariate case that throws away temporal information, we want to solve the BC task with a time-series probability model. A simple example would help to shed light on what we want from a time-series probability model.

Consider the following example: Imagine the heatwave duration is consistently two times longer in the climate model than it is in the observational record. We can then manually construct a probability model. Our probability model copies the climate model trajectory; if the trajectory passes above 30°C for multiple days in a row, cut the trajectory in half and add a bias  $a$  and some noise,  $\epsilon_t$ , to get the corresponding estimated observation; otherwise, assign 0.

There are two main things to notice from this probability model: a) the value at time point  $t_i$ ,  $y_{t_i}^o$ , is some deterministic function  $f$  of the ordered future values  $y_{t_j \geq t_i}^g$  from the climate model (the notation  $j \geq i$  denotes all indices greater or equal to  $i$ ), and b) since the probability model has some noise,  $\epsilon_t$ , we can sample different values for  $y_{t_i}^o$  for each  $t_i$ , leading to an ensemble of trajectories. In ML, we call the readouts from the sampling procedure the inference stage (for more details, see discussion below).

Since  $\epsilon_t$  comes from the Normal distribution, we can concisely write our model as

$$Y_{t_k}^o | inp_k \sim \text{Normal}(f(inp_k), \sigma^2) \quad (1)$$

where  $inp_k := \{y_{t_k:t_M}^g, t_k\}$ , with the notation  $t_i : t_j$  to indicate all time-points between  $t_i$  and  $t_j$  included. That is, again, an easy probability model with a learnable parameter  $a$  which we can learn using standard linear regression libraries. (See Appendix, Algorithm 3 for an example implementation for this probability model and Figure 15 for an illustration.)

An obvious extension to the simple time-series probability model above is to a) add past values from the climate model, b) add past observations, and c) choose the function  $f$  as a neural network parameterised by  $\theta$ . So, our proposed probability model is:

$$Y_{t_k}^o | inp_k \sim \text{Normal}(f_\theta(inp_k), g_\theta(inp_k)) \quad (2)$$

here  $Y_{t_k}^o$  are random variables representing the temperatures at time  $t_k$  for observations, where we have  $t_1 < \dots < t_k < \dots < t_M$  with  $M$  being the size of the sequence. Additionally, we define  $inp_k := (y_{t_1:t_M}^g, y_{t_1:t_{k-1}}^o, t_1^g : t_M^g, t_1^o : t_{k-1}^o)$ ,  $f_\theta$  and  $g_\theta$  are functions with parameters represented by  $\theta$ .

We think this probability model will perform better (than existing bias-correction models) on correction tasks that aim to extract temporal statistics. First, it considers the dependencies of past observations. Second, it considers past and future climate model outputs. Third, unlike univariate BC, it does not require any collapse or aggregation of data – allowing the model to learn from more data. Lastly, the model also has the theoretical ability to overcome the time sync issue which Maraun describes [27] as following: “But crucially, and different to numerical weather forecasts, transient climate simulations are not in synchrony with observations. As a result, regression models cannot easily be calibrated. Therefore, researchers explored possibilities to bias correct based on long-term distributions instead of day-to-day relationships”. Since our probability model considers past observations and (past, future) climate model outputs, there is no need to rely on “day-to-day” relationships. We have shown an example of this in Equation 1.

In ML, once we have a probability model, we need to choose the architecture that would enable the learning of the model’s parameters. In this case, we have chosen the Taylorformer [29], which is an adaptation of the Transformer attention model by Vaswani [44] to real-valued targets on a continuum. We now turn to explain the adaptations needed for the BC task.

### 3.3. From probability model to ML implementation

We now turn to explain the adaptations needed for the BC task. To implement the Taylorformer (or any deep learning model), we have to set a training objective and then construct a training dataset, a hold-out set, and an inference procedure.

*Training objective.* Our training objective is illustrated in Figure 1. Our aim is to correct future observations (dashed purple line) given a pair of sequences: one sequence of past observations (solid blue line) and another sequence of past and future climate model outputs (solid red line). Hereafter, we term the set of points either in past observations or in (past, future) climate model outputs the context set and

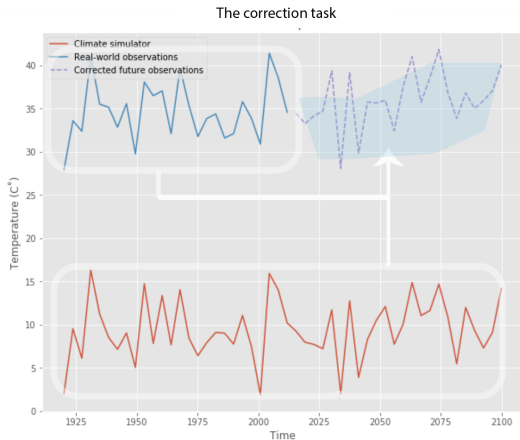


**Figure 1.** An illustration of the training objective. Our goal is to correct for future observations (dashed purple line) given all the data bounded by the white rectangles. See main text for details..

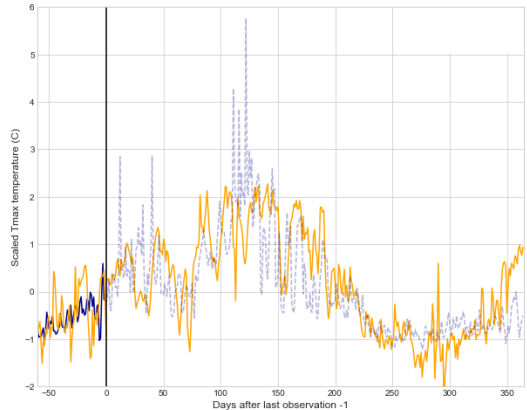


**Figure 2.** An example of a pair of (climate model, observation) trajectories extracted to train our ML model. Here, the climate model (solid orange line) and past observations (solid blue line) are used to correct for the 365 daily unseen values (dashed light-blue line)..

denote it by  $C$ . Based on  $C$ , we correct the unknown values (dashed purple line), which we collectively term the target set, denoted by  $T$ .

In probabilistic language, we maximise the log-likelihood of the unseen values (dashed purple line) given the input (maximum likelihood is the same objective as in the univariate case). Mathematically, using the notation from above, this means

$$\max_{\theta} \text{Log } p(\mathbf{Y}_{\mathbf{t}; i \in \mathbf{T}^o} | \text{inp}_{k: k \in C}, \theta) \quad (3)$$

**Training dataset.** Practically, to train our dataset for our objective, we must do more than feed in the entire trajectory of the pair (observations, climate model) from 1948-1988 since this would enable only one gradient descent pass, and little learning would occur. Hence, we have to break down the pair into many pairs with a similar structure, as shown in Figure 2.

Furthermore, We have to address the following three issues that occur with the constructed training set in Figure 2 and with our objective. (1) we want to allow pairs to have differing lengths — it is unclear a-priori which length is optimal, and (2) we do not want to assume any independence between random variables in our objective (assuming independence would limit our ability to learn temporal structures). Our only way to do that is to learn our model auto-regressively. (3) if our model is auto-regressive, we have to heed that it does not learn the rule “Tomorrow will be the same as today” as pointed out by Nivron et al. [29]. To address (1) and (2), we will use the Taylorformer [29] architecture fitting the auto-regressive model for arbitrary length sequences. We now describe the concrete pairs in our training set and then refine it to handle concern (3).

Our training sequences follow the exact construction of the probability model. However, when correcting  $Y_{t_k}^o$  instead of taking the full length  $M$  of the climate model sequence and all previous observations up to  $k$  (excluding) when constructing  $\text{inp}_k$ , we slice snapshots of shorter lengths. The length of the pair of sequences is chosen randomly (addressing point (1) above) for each row, and the starting position  $t_1$  is changing as well to avoid learning a prediction instead of a correction (this point is explained in the discussion at the end of this section). An explicit example of a row in our dataset is:  $[(t_1, y_{1,t_1}, 1, 0), \dots (t_N, y_{1,t_N}, 1, 0), (t_1, y_{0,t_1}, 0, 8) \dots (t_N, y_{0,t_N}, 0, 8) \dots (t_{N+B}, y_{0,t_{N+B}}, 0, 8)]$ . The

entries of each tuple are of the form  $(t_j, y_{k,t_j}, k, r)$  where  $k$  equals 1 if the value is from the observation time-series and 0 if it is from the climate model time-series and  $r$  indicates the initial-condition run index, with 0 referring to observations.

*Changing context and target lengths and max length.* To address the problem of auto-regressive models, which sometimes are just copying machines of the previous input (as explained in 3.3), we employ the following mechanism: The context and target sets' sizes are changing with different spacing between values (irregular grid). This follows the work in Taylorformer [29], encouraging the network to learn more robust predictions. Further, we limit the maximum sequence length to 360 points, which is chosen to address the high computational load of attention blocks. (See implementation in Algorithm 1).

*Hold-out set.* We must split the training data and holdout set to an extensive time range to show our model's performance in a changing climate and have enough data to make statements about climate-related statistics. Therefore, we split the training data between 1948 and 1988, and the holdout was set between 1989 and 2008.

*Inference.* In ML, we first train a model to learn the parameters of a network. Once the parameters are learned using an objective (here, maximum likelihood), they are fixed and we can use the network to get our desired readouts. This is called the inference stage, and for our chosen sequential model, it operates in a generative mode. While in training, we try to predict the mean and standard deviation of the Normal distribution as stated in 2, in a generative mode, we sample from that distribution. To predict the next value, we first attach the sampled value to the new  $inp_k$  sequence to predict the next value and then proceed. In training, we attach the actual value (as opposed to a sampled value or predicted value) to the new  $inp_k$  sequence — this is the standard way to train a sequential model using maximum likelihood.

Our sampling (inference) process mimics the way we trained the model — we feed in a sequence of size 180, with the last 60 days of 1988 for observations and the climate model outputs and the next 120 days of 1989 from the climate model to produce the first estimated observation of 1989. Next, we attach the sampled value to our observations and shift all the processes by one day to the right so that when sampling the second day of 1989, we still have a context sequence of size 180. We iterate the process until we have all days up to 2008. (See implementation in Algorithm 2).

### 3.4. Discussion: other ways to slice and infer the data

#### 3.4.1. Slicing discussion

It is not trivial to slice the pair of (climate model, observations) sequences to build a training corpus. For example, the corpus has to encourage the correction task instead of a prediction task. If we give the model pairs of (climate model  $i$ , obs) at time  $t$  with different initial-condition indexed by  $i$ , then the ML model will learn to ignore the climate model completely; the observation value would always be the same for all pairs while the climate model output would keep on changing based on which initial-condition  $i$  was chosen and hence uninformative.

Given the understanding that we have to make our pairing process in an educated manner, how should we pair the climate model(s) with observations? This is only possible, if we make some assumptions about the generating process.

Here are a few possibilities for sensible corpus constructions:

1.  $(Y_{1,loc_1}^g, Y_{loc_1}^o), (Y_{2,loc_2}^g, Y_{loc_2}^o), \dots$
2.  $(Y_{1,loc_1,t1:t2}^g, Y_{loc_1,t1:t2}^o), (Y_{2,loc_1,t3:t4}^g, Y_{loc_1,t3:t4}^o), \dots$

In option (1),  $Y_{i,loc_j}^g$  is the climate model with the initial-condition indexed by  $i$  and obtained from geographical region indexed by  $j$ . We pair such a sequence with  $Y_{loc_j}^o$ , the observed sequence from



the same region. This setup assumes that the correction is the same for repeated patterns for different regions and initial-condition runs and the full trajectory of the sequences. In option (2),  $Y_{i,loc_j,s}^g$  is the climate model for time-window  $s$  and is paired with  $Y_{loc_j,s}^o$ , the observed sequence from same time-window. Here, the region does not change throughout the corpus, but the time-window and initial-condition index do. Given a repeated pattern, it assumes that the same correction applies only to one specific region for different time-windows and different initial-condition runs.

These setups are selected examples of slicing the data. The question remains: Which possibility can be chosen to construct the corpus? A standard ML procedure is to choose the model that performed best on hold-out likelihood and this is how we chose our slicing above.

### 3.4.2. Inference discussion

We could have used different setups to execute the sampling (generation) process, and not all generation processes are equal. It is a matter of empirical work to choose the generation process. Our choice above is a convenient choice to align with the training procedure. For example, we can inject the entire trajectory of a climate model run and all observations from 1948-1988 and sample day-by-day values up until 2008. Alternatively, we can use the same inputs to generate in non-chronological order, generate the 1st of January 1989, and then fill in the values in-between before continuing to 1990 and further.

## 4. Experiments

To test our model, we do the following experiment: First, we bias-correct daily maximum temperatures for Abuja, Nigeria, and separately for Tokyo, Japan, for 1989-2008 based on the years 1948-1988. Second, we calculate the heatwave duration distribution from the bias-corrected data.

We compare our model to the raw output from the climate model and to three BC methods: mean correction, mean and variance correction, and EQM. Table 1 shows the RMSE obtained by each BC method – our temporal BC achieves 26% lower RMSE in Tokyo, Japan, and 22% lower in Abuja, Nigeria.

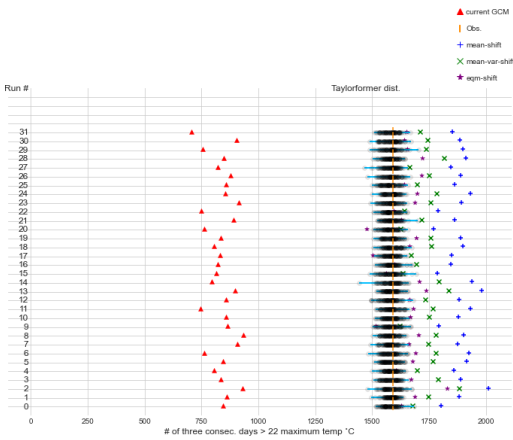
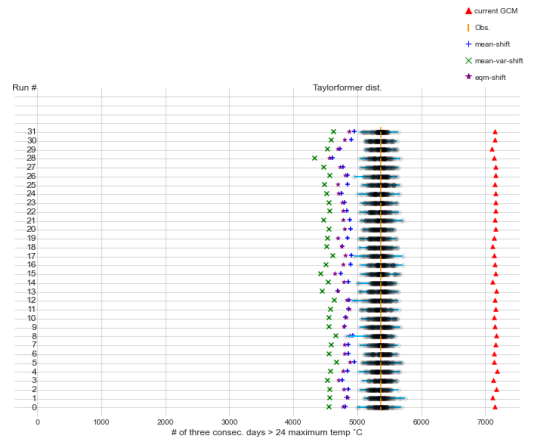
Figure 3 shows the results for the calculated heatwave duration distribution for Tokyo, Japan using a heatwave threshold of three consecutive days above 22°C maximum temperature. The raw outputs from the IPSL climate model (red triangles) underestimate the number of instances of observed heatwaves (vertical orange line) by more than 100% for the period 1989 – 2008. Our novel Taylorformer temporal BC produces a much more accurate distribution (horizontal box-plots) per run (0-31) for the number of heatwaves in the same period with an ensemble average differing by at most 1% from the observed number of heatwaves. Other BC models perform worse: 24%, 18%, 15% for mean-shift (‘+’), mean and variance shift (‘X’), and EQM (‘★’), respectively.

Figure 4 shows the results for Abuja, Nigeria using a heatwave threshold of three consecutive days above 24°C maximum temperature. The raw outputs from the IPSL climate model (red triangles) overestimate the number of instances of observed heatwaves (vertical orange line) by more than 33% for the period 1989 – 2008. Our novel Taylorformer temporal BC produces a much more accurate distribution (horizontal box-plots) per run (0-31) for the number of heatwaves in the same period with an ensemble average differing by at most 1% from the observed number of heatwaves. Other BC models perform worse: 14%, 19%, 15% for mean-shift (‘+’), mean and variance shift (‘X’), and EQM (‘★’), respectively.

At both locations our model’s ensemble average differs by at most 1% from the actual observed values, whereas the other BC models differ by 15 – 24% and 14 – 19% for Tokyo and Abuja, respectively. Similar figures (using different heatwave thresholds), found in appendix C, show that our model consistently outperforms the other BC alternatives.

**Table 1.** Our Temporal BC outperforms alternative BC on the RMSE for the daily maximum temperature values ( $^{\circ}\text{C}$ ) for the 20-year period from 1989-2008.

Model	RMSE	
	Tokyo	Abuja
Climate model	6.29	3.33
Temporal BC	2.57	1.88
EQM	3.49	2.42
Mean	3.80	2.77
Mean + Var	3.50	2.69

**Figure 3.** Number of periods of three consecutive days above  $22^{\circ}\text{C}$  maximum temperature in Tokyo, Japan for the period 1989–2008. IPSL climate model (red triangles), observations (vertical orange line), Taylorformer temporal BC (horizontal box-plots), mean-shift ('+'), mean and variance shift ('X'), and EQM ('★').**Figure 4.** Number of periods of three consecutive days above  $24^{\circ}\text{C}$  maximum temperature in Abuja, Nigeria for the period 1989–2008. IPSL climate model (red triangles), observations (vertical orange line), Taylorformer temporal BC (horizontal box-plots), mean-shift ('+'), mean and variance shift ('X'), and EQM ('★').

## 5. Conclusion

This paper offers the first BC method to extract long-range temporal properties, such as heatwave duration statistics, from climate models. It is done by first re-thinking BC as a probability model rather than an algorithmic procedure and then combining it with attention ML models. Our temporal BC model is tested on the correction of time series in Abuja, Nigeria, and Tokyo, Japan, and the results yield much more accurate heatwave duration statistics than have been achieved hitherto. Our model opens up the opportunity to do BC temporally. Going forward, this study needs to be scaled-up, considering multiple regions, more climate models, more climate statistics and extrapolations to the future climate (e.g., up to 2050).

**Funding Statement.** This research was supported by the Artificial Intelligence for Environmental Risks (AI4ER) CDT, University of Cambridge.

**Competing Interests.** None

**Data Availability Statement.** All data and code is open-sourced and available: IPSL climate model (data) – <https://esgf-node.llnl.gov/search/cmip6/>, NCEP-NCAR Reanalysis 1 (data) – <https://psl.noaa.gov/data/gridded/data.ncep.reanalysis>.



html, ERA5 (data) <https://www.ecmwf.int/en/forecasts/dataset/ecmwf-reanalysis-v5>, Taylorformer temporal BC model (code) –<https://github.com/oremnirv/Taylorformer>

**Ethical Standards.** The research meets all ethical guidelines, including adherence to the legal requirements of the study country.

**Author Contributions.** **Omer Nivron:** Conceptualization, Methodology, Writing- Original draft preparation, Investigation, Visualization, Software, Formal analysis. **Damon Wischik:** Conceptualization, Formal analysis, Methodology, Writing- Reviewing and Editing. **Mathieu Vrac:** Writing- Reviewing and Editing, Validation, Supervision. **Emily Shuckburgh:** Writing- Reviewing and Editing, Supervision. **Alexander Archibald:** Writing- Reviewing and Editing, Supervision.

**Supplementary Material.** Additional figures and implementation algorithms are provided in appendices A-D.

## References

- [1] Tamara Ben Ari. “Causes and implications of the unforeseen 2016 extreme yield loss in France’s breadbasket”. In: 2020. URL: <https://api.semanticscholar.org/CorpusID:235024720>.
- [2] Céline Bellard et al. “Impacts of climate change on the future of biodiversity”. In: *Ecology Letters* 15.4 (2012), pp. 365–377. DOI: <https://doi.org/10.1111/j.1461-0248.2011.01736.x>. eprint: <https://onlinelibrary.wiley.com/doi/pdf/10.1111/j.1461-0248.2011.01736.x>. URL: <https://onlinelibrary.wiley.com/doi/abs/10.1111/j.1461-0248.2011.01736.x>.
- [3] F. Boberg and J. Christensen. “Overestimation of Mediterranean summer temperature projections due to model deficiencies”. In: *Nature Climate Change* 2 (2012), pp. 433–436.
- [4] Julien Boé et al. “Statistical and dynamical downscaling of the Seine basin climate for hydro-meteorological studies”. In: *International Journal of Climatology* 27 (2007). URL: <https://api.semanticscholar.org/CorpusID:128643024>.
- [5] Olivier Boucher et al. “Presentation and Evaluation of the IPSL-CM6A-LR Climate Model”. In: *Journal of Advances in Modeling Earth Systems* 12.7 (2020). e2019MS002010 10.1029/2019MS002010, e2019MS002010. DOI: <https://doi.org/10.1029/2019MS002010>. eprint: <https://agupubs.onlinelibrary.wiley.com/doi/pdf/10.1029/2019MS002010>. URL: <https://agupubs.onlinelibrary.wiley.com/doi/abs/10.1029/2019MS002010>.
- [6] Alex Cannon. “Multivariate quantile mapping bias correction: an N-dimensional probability density function transform for climate model simulations of multiple variables”. In: *Climate Dynamics* 50 (Jan. 2018). DOI: 10.1007/s00382-017-3580-6.
- [7] Jens Hesselbjerg Christensen et al. “On the need for bias correction of regional climate change projections of temperature and precipitation”. In: *Geophysical Research Letters* 35 (2008). URL: <https://api.semanticscholar.org/CorpusID:128752652>.
- [8] Niklas S. Christensen et al. “The Effects of Climate Change on the Hydrology and Water Resources of the Colorado River Basin”. In: *Climatic Change* 62 (2004), pp. 337–363. URL: <https://api.semanticscholar.org/CorpusID:53533021>.
- [9] Ph Ciais et al. “Europe-wide reduction in primary productivity caused by the heat and drought in 2003”. In: *Nature* 437 (Oct. 2005), pp. 529–33. DOI: 10.1038/nature03972.
- [10] Dimitri DeFrance et al. “Consequences of rapid ice sheet melting on the Sahelian population vulnerability”. In: *Proceedings of the National Academy of Sciences* 114.25 (2017), pp. 6533–6538. DOI: 10.1073/pnas.1619358114. eprint: <https://www.pnas.org/doi/pdf/10.1073/pnas.1619358114>. URL: <https://www.pnas.org/doi/abs/10.1073/pnas.1619358114>.
- [11] Léonard Dekens et al. “Multivariate distribution correction of climate model outputs: A generalization of quantile mapping approaches”. In: *Environmetrics* 28 (2017). URL: <https://api.semanticscholar.org/CorpusID:126106313>.
- [12] Michel Déqué. “Frequency of precipitation and temperature extremes over France in an anthropogenic scenario: Model results and statistical correction according to observed values”. In: *Global and Planetary Change* 57 (2007), pp. 16–26. URL: <https://api.semanticscholar.org/CorpusID:128409261>.
- [13] Jonathan M. Eden et al. “Skill, Correction, and Downscaling of GCM-Simulated Precipitation”. In: *Journal of Climate* 25 (2012), pp. 3970–3984. URL: <https://api.semanticscholar.org/CorpusID:128629641>.
- [14] V. Eyring et al. “Overview of the Coupled Model Intercomparison Project Phase 6 (CMIP6) experimental design and organization”. In: *Geoscientific Model Development* 9.5 (2016), pp. 1937–1958. DOI: 10.5194/gmd-9-1937-2016. URL: <https://gmd.copernicus.org/articles/9/1937/2016/>.
- [15] Bastien François et al. “Multivariate bias corrections of climate simulations: which benefits for which losses?” In: 2020.
- [16] Peter H. Gleick. “Climate change, hydrology, and water resources”. In: *Reviews of Geophysics* 27 (1989), pp. 329–344. URL: <https://api.semanticscholar.org/CorpusID:128418811>.
- [17] S. Hagemann et al. “Impact of a Statistical Bias Correction on the Projected Hydrological Changes Obtained from Three GCMs and Two Hydrology Models”. In: *Journal of Hydrometeorology* 12 (2011), pp. 556–578.
- [18] E. Hawkins et al. “Calibration and bias correction of climate projections for crop modelling: An idealised case study over Europe”. In: *Agricultural and Forest Meteorology* 170 (2013), pp. 19–31.
- [19] Hans Hersbach et al. “The ERA5 global reanalysis”. In: *Quarterly Journal of the Royal Meteorological Society* (May 2020). DOI: 10.1002/qj.3803.
- [20] Chun Kit Ho et al. “Calibration strategies a source of additional uncertainty in climate change projections”. In: *Bulletin of the American Meteorological Society* (2012). ISSN: 00030007. DOI: 10.1175/2011BAMS3110.1.

- [21] Frédéric Hourdin et al. “LMDZ6A: The Atmospheric Component of the IPSL Climate Model With Improved and Better Tuned Physics”. In: *Journal of Advances in Modeling Earth Systems* 12.7 (2020). e2019MS001892 10.1029/2019MS001892, e2019MS001892. DOI: <https://doi.org/10.1029/2019MS001892>. eprint: <https://agupubs.onlinelibrary.wiley.com/doi/pdf/10.1029/2019MS001892>. URL: <https://agupubs.onlinelibrary.wiley.com/doi/abs/10.1029/2019MS001892>.
- [22] T. Iizumi, M. Yokozawa, and M. Nishimori. “Probabilistic evaluation of climate change impacts on paddy rice productivity in Japan”. In: *Climatic Change* 107 (2011), pp. 391–415.
- [23] Malaak Kallache et al. “Nonstationary probabilistic downscaling of extreme precipitation”. In: *Journal of Geophysical Research* 116 (2010). URL: <https://api.semanticscholar.org/CorpusID:67764166>.
- [24] Eugenia Kalnay et al. “The NCEP/NCAR 40-Year Reanalysis Project”. In: *Renewable Energy* (1996). URL: <https://api.semanticscholar.org/CorpusID:124135431>.
- [25] Haibin Li, J. Sheffield, and E. Wood. “Bias correction of monthly precipitation and temperature fields from Intergovernmental Panel on Climate Change AR4 models using equidistant quantile matching”. In: *Journal of Geophysical Research* 115 (2010).
- [26] Thibaut Lurton et al. “Implementation of the CMIP6 Forcing Data in the IPSL-CM6A-LR Model”. In: *Journal of Advances in Modeling Earth Systems* 12.4 (2020). e2019MS001940 10.1029/2019MS001940, e2019MS001940. DOI: <https://doi.org/10.1029/2019MS001940>. eprint: <https://agupubs.onlinelibrary.wiley.com/doi/pdf/10.1029/2019MS001940>. URL: <https://agupubs.onlinelibrary.wiley.com/doi/abs/10.1029/2019MS001940>.
- [27] Douglas Maraun. *Bias Correcting Climate Change Simulations - a Critical Review*. 2016. DOI: 10.1007/s40641-016-0050-x.
- [28] Camilo Mora et al. “Global risk of deadly heat”. In: *Nature Climate Change* 7 (June 2017). DOI: 10.1038/nclimate3322.
- [29] Omer Nivron, Raghul Parthipan, and Damon Wischik. “Taylorformer: Probabilistic Predictions for Time Series and other Processes”. In: *ArXiv abs/2305.19141* (2023). URL: <https://api.semanticscholar.org/CorpusID:258967520>.
- [30] C. H. O’Reilly, D. J. Befort, and A. Weisheimer. “Calibrating large-ensemble European climate projections using observational data”. In: *Earth System Dynamics* 11.4 (2020), pp. 1033–1049. DOI: 10.5194/esd-11-1033-2020. URL: <https://esd.copernicus.org/articles/11/1033/2020/>.
- [31] OECD. *The Economic Consequences of Climate Change*. 2015, p. 140. DOI: <https://doi.org/https://doi.org/10.1787/9789264235410-en>. URL: <https://www.oecd-ilibrary.org/content/publication/9789264235410-en>.
- [32] T. N. Palmer and Antje Weisheimer. “Diagnosing the causes of bias in climate models – why is it so hard?” In: *Geophysical & Astrophysical Fluid Dynamics* 105.2-3 (2011), pp. 351–365. DOI: 10.1080/03091929.2010.547194. eprint: <https://doi.org/10.1080/03091929.2010.547194>. URL: <https://doi.org/10.1080/03091929.2010.547194>.
- [33] C. Pianì and J. O. Haerter. “Two dimensional bias correction of temperature and precipitation copulas in climate models”. In: *Geophysical Research Letters* 39.20 (2012). DOI: <https://doi.org/10.1029/2012GL053839>. eprint: <https://agupubs.onlinelibrary.wiley.com/doi/pdf/10.1029/2012GL053839>. URL: <https://agupubs.onlinelibrary.wiley.com/doi/abs/10.1029/2012GL053839>.
- [34] Shilong Piao et al. “The impacts of climate change on water resources and agriculture in China”. In: *Nature* 467 (2010), pp. 43–51. URL: <https://api.semanticscholar.org/CorpusID:4410647>.
- [35] Y. Robin et al. “Multivariate stochastic bias corrections with optimal transport”. In: *Hydrology and Earth System Sciences* 23.2 (2019), pp. 773–786. DOI: 10.5194/hess-23-773-2019. URL: <https://hess.copernicus.org/articles/23/773/2019/>.
- [36] K. Salvi, S. Kannan, and S. Ghosh. “Statistical Downscaling and Bias Correction for Projections of Indian Rainfall and Temperature in Climate Change Studies”. In: *International Journal of Climatology* 26 (2006). URL: <https://api.semanticscholar.org/CorpusID:128686717>.
- [37] D. Stainforth et al. “Confidence, uncertainty and decision-support relevance in climate predictions”. In: *Philosophical Transactions of the Royal Society A: Mathematical, Physical and Engineering Sciences* 365 (2007), pp. 2145–2161.
- [38] Claudia Teutschbein et al. “Bias correction of regional climate model simulations for hydrological climate-change impact studies: Review and evaluation of different methods”. In: *Journal of Hydrology* 456 (2012), pp. 12–29. URL: <https://api.semanticscholar.org/CorpusID:129017016>.
- [39] M. Themeßl, A. Gobiet, and A. Leuprecht. “Empirical-statistical downscaling and error correction of daily precipitation from regional climate models”. In: *International Journal of Climatology* 31 (2011), pp. 1530–1544.
- [40] Richard S. J. Tol. “The Economic Impact of Weather and Climate”. In: *Climate Action eJournal* (2021). URL: <https://api.semanticscholar.org/CorpusID:228207225>.
- [41] Richard S. J. Tol. “The Economic Impacts of Climate Change”. In: *Review of Environmental Economics and Policy* 12 (2018), pp. 4–25. URL: <https://api.semanticscholar.org/CorpusID:159009492>.
- [42] M. Turco et al. “Bias correction and downscaling of future RCM precipitation projections using a MOS-Analog technique”. In: *Journal of Geophysical Research* 122 (2017), pp. 2631–2648.
- [43] Ashish Vaswani et al. “Attention is all you need”. In: *Advances in Neural Information Processing Systems*. 2017.
- [44] M. Vrac. “Multivariate bias adjustment of high-dimensional climate simulations: the Rank Resampling for Distributions and Dependences ( $R^2D^2$ ) bias correction”. In: *Hydrology and Earth System Sciences* 22.6 (2018), pp. 3175–3196. DOI: 10.5194/hess-22-3175-2018. URL: <https://hess.copernicus.org/articles/22/3175/2018/>.

- [46] M. Vrac and S. Thao. “R<sup>2</sup>D<sup>2</sup> v2.0: accounting for temporal dependences in multivariate bias correction via analogue rank resampling”. In: *Geoscientific Model Development* 13.11 (2020), pp. 5367–5387. DOI: 10.5194/gmd-13-5367-2020. URL: <https://gmd.copernicus.org/articles/13/5367/2020/>.
- [47] M. Vrac et al. “Dynamical and statistical downscaling of the French Mediterranean climate: uncertainty assessment”. In: *Natural Hazards and Earth System Sciences* 12.9 (2012), pp. 2769–2784. DOI: 10.5194/nhess-12-2769-2012. URL: <https://nhess.copernicus.org/articles/12/2769/2012/>.
- [48] A. Wood et al. “Long-range experimental hydrologic forecasting for the eastern United States”. In: *Journal of Geophysical Research* 107 (2002), p. 4429.
- [49] Chong-yu Xu. “From GCMs to river flow: a review of downscaling methods and hydrologic modelling approaches”. In: *Progress in Physical Geography: Earth and Environment* 23.2 (1999), pp. 229–249. DOI: 10.1177/030913339902300204. eprint: <https://doi.org/10.1177/030913339902300204>. URL: <https://doi.org/10.1177/030913339902300204>.

## A. Linear regression mean shift derivation

Estimation of the parameters in linear regression is done using maximum likelihood as the objective. Using maximum likelihood and denoting  $\mathbf{Y}^g$  to refer to the set of all climate model outputs we have

$$\begin{aligned}
 \max_{\theta} P(y_{t_1}^o, \dots, y_{t_N}^o | \mathbf{Y}^g) &\stackrel{\text{independence}}{=} \prod_{i=1}^N P(y_{t_i}^o | y_{t_i}^g) \\
 &\stackrel{\text{normal r.v.}}{=} \prod_{i=1}^N \frac{1}{\sqrt{2\pi\sigma^2}} \exp\left(-\frac{(y_{t_i}^o - y_{t_i}^g - c)^2}{2\sigma^2}\right) \\
 &\xrightarrow{\log} \sum_{i=1}^N \log(1) - \log\sqrt{2\pi\sigma^2} - \frac{(y_{t_i}^o - y_{t_i}^g - c)^2}{2\sigma^2} \tag{A.1} \\
 \frac{\partial}{\partial c} \xrightarrow{\text{derivative}=0} &-\sum_{i=1}^N (y_{t_i}^o - y_{t_i}^g - c) = 0 \\
 c &= \frac{1}{N} \sum_{i=1}^N y_{t_i}^o - \frac{1}{N} \sum_{i=1}^N y_{t_i}^g
 \end{aligned}$$

## B. Algorithmic implementation

## C. Additional experimental results

### C.1. Tokyo, Japan

Figure 5 shows the results for Tokyo, Japan using a heatwave threshold of three consecutive days above 18°C maximum temperature. The raw outputs from the IPSL climate model (red triangles) underestimate the number of instances of observed heatwaves (vertical orange line) for the period 1989 – 2008. Our novel Taylorformer temporal BC produces a much more accurate distribution (horizontal box-plots) per run (0-31) for the number of heatwaves in the same period with an ensemble average differing by at most 1% from the observed number of heatwaves. Other BC models perform worse: 7%, 6%, 6% for mean-shift (+), mean and variance shift (X), and EQM (★), respectively.

Figure 6 shows the results for Tokyo, Japan using a heatwave threshold of three consecutive days above 20°C maximum temperature. The raw outputs from the IPSL climate model (red triangles) underestimate the number of instances of observed heatwaves (vertical orange line) for the period 1989 – 2008. Our novel Taylorformer temporal BC produces a much more accurate distribution (horizontal box-plots) per run (0-31) for the number of heatwaves in the same period with an ensemble average differing by at most 1.4% from the observed number of heatwaves. Other BC models perform worse: 15%, 9%, 8% for mean-shift (+), mean and variance shift (X), and EQM (★), respectively.

Figure 7 shows the results for Tokyo, Japan using a heatwave threshold of three consecutive days above 24°C maximum temperature. The raw outputs from the IPSL climate model (red triangles) underestimate the number of instances of observed heatwaves (vertical orange line) for the period 1989 – 2008. Our novel Taylorformer temporal BC produces a much more accurate distribution (horizontal box-plots) per run (0-31) for the number of heatwaves in the same period with an ensemble average differing by at most 3% from the observed number of heatwaves. Other BC models perform worse: 23%, 12%, 11% for mean-shift (+), mean and variance shift (X), and EQM (★), respectively.

Figure 8 shows the results for Tokyo, Japan using a heatwave threshold of three consecutive days above 26°C maximum temperature. The raw outputs from the IPSL climate model (red triangles) underestimate the number of instances of observed heatwaves (vertical orange line) for the period 1989 – 2008. Our novel Taylorformer temporal BC produces a much more

**Algorithm 1** Generate Data Batches from Sequences

**Require:** one sequences  $Y^o$  (observations) and  $K$  sequences  $Y^g$  (climate model outputs for  $K$  initial-conditions), timestamp sequence  $t' = \{t'_1, \dots, t'_M\}$   $\triangleright Y^o \in \mathbf{R}^M, Y^g \in \mathbf{R}^{K \times M}, t' \in \mathbf{N}^M$  : for all  $i, t'_i := \text{day of year}(t_i)$

**Ensure:** Two arrays:  $Y_C$  (context set) and  $Y_T$  (target set) of size  $S$

```

1: while size of  $(Y_C, Y_T) < S$  do
2:    $k \leftarrow$  random selection from  $\{1, \dots, K\}$ 
3:    $i \leftarrow$  random selection from  $\{1, \dots, M\}$ 
4:    $|C|, |T| \leftarrow$  random sizes for context and target sets
5:   Initialize sequences  $Seq^o, Seq^g$  with size  $|C| + |T|$ 
6:   for  $j \leftarrow i$  to  $i + |C| + |T| - 1$  do
7:      $Seq^o[j] \leftarrow (Y^o[j], t'[j], 0)$ 
8:      $Seq^g[j] \leftarrow (Y^g_k[j], t'[j], 1)$ 
9:   end for
10:  Subsample and Sort  $Seq^o, Seq^g$   $\triangleright$  Randomly subsample points and sort
11:   $Y_C \leftarrow$  concatenate indices in  $C$  from  $Seq^o$  with indices in  $C \cup T$  from  $Seq^g$ 
12:   $Y_T \leftarrow$  values from  $Seq^o$  not in  $C$ 
13: end while
14: return  $Y_C, Y_T$ 

```

**Algorithm 2** Inference with Trained Model

**Require:**

A trained model  $M$   
Sequence  $Y^g$  of climate model predictions  
Sequence  $Y^o$  of observations  
Target sequence size  $|N|$

**Ensure:**

Extended sequence  $Y^o$  with predicted values until  $|Y^o| = |N|, |Y^g| = |N| + 120$

```

1: Initialize  $i = 1$ 
2: Choose  $k$  from  $[1, \dots, K]$ 
3: while  $|Y^o| < |N|$  do
4:    $X_g \leftarrow$  select 180 consecutive points from  $Y^g_k$  starting at  $t'_i$ 
5:    $X_o \leftarrow$  select 60 consecutive points from  $Y^o$  starting at  $t'_i$ 
6:    $X \leftarrow$  concatenate  $X_g$  and  $X_o$ 
7:    $(\mu, \sigma) \leftarrow M(X)$   $\triangleright$  Model  $M$  predicts parameters
8:    $y^o_{\text{new}} \leftarrow$  sample from  $\mathcal{N}(\mu, \sigma)$ 
9:   Append  $y^o_{\text{new}}$  to  $Y^o$ 
10:   $i \leftarrow i + 1$ 
11: end while

```

accurate distribution (horizontal box-plots) per run (0-31) for the number of heatwaves in the same period with an ensemble average differing by at most 8.6% from the observed number of heatwaves. Other BC models perform worse: 30%, 21%, 22% for mean-shift ('+'), mean and variance shift ('X'), and EQM ('\*'), respectively.

Figure 9 shows the results for Tokyo, Japan using a heatwave threshold of three consecutive days above 28°C maximum temperature. The raw outputs from the IPSL climate model (red triangles) underestimate the number of instances of observed heatwaves (vertical orange line) for the period 1989 – 2008. Our novel Taylorformer temporal BC produces a much more accurate distribution (horizontal box-plots) per run (0-31) for the number of heatwaves in the same period with an ensemble average differing by at most 20% from the observed number of heatwaves. Other BC models perform worse: 83%, 66%, 65% for mean-shift ('+'), mean and variance shift ('X'), and EQM ('\*'), respectively.

**Algorithm 3** Compute  $y_o$  Based on Conditions Applied to  $y_g$ 


---

```

1: Generate time series  $t$  from 0 to 10 with 500 linearly spaced points.
2:  $y_g \leftarrow 30 + 15 \sin(2\pi \times 0.6 \times t)$ .
3:  $a \leftarrow 2.2$ .
4: Initialize  $y_o$  as an empty list.
5:  $x_g \leftarrow (y_g \geq 30)$ .
6: Prepend and append 0 to  $x_g$ .
7:  $\delta_{x_g} \leftarrow$  compute the difference between consecutive elements in  $x_g$ .
8:  $start\_end \leftarrow$  find indices where  $\delta_{x_g} \neq 0$ .
9:  $\delta_{start\_end} \leftarrow$  compute the difference between consecutive elements in  $start\_end$ .
10: for  $i = 0$  to  $len(y_g) - 1$  do
11:    $cond \leftarrow$  False.
12:   for  $k = 0$  to  $len(start\_end) - 2$  do
13:     if  $i \geq start\_end[k]$  and  $i < start\_end[k] + \frac{\delta_{start\_end}[k]}{2}$  and  $\delta_{x_g}[start\_end[k]] == 1$ 
and  $\delta_{x_g}[start\_end[k+1]] == -1$  then
14:        $y_o.append(30 + a + \text{Normal}(0, \sigma^2))$ .
15:        $cond \leftarrow$  True.
16:       break.
17:     end if
18:   end for
19:   if  $cond ==$  False then
20:      $y_o.append(0)$ .
21:   end if
22: end for

```

---

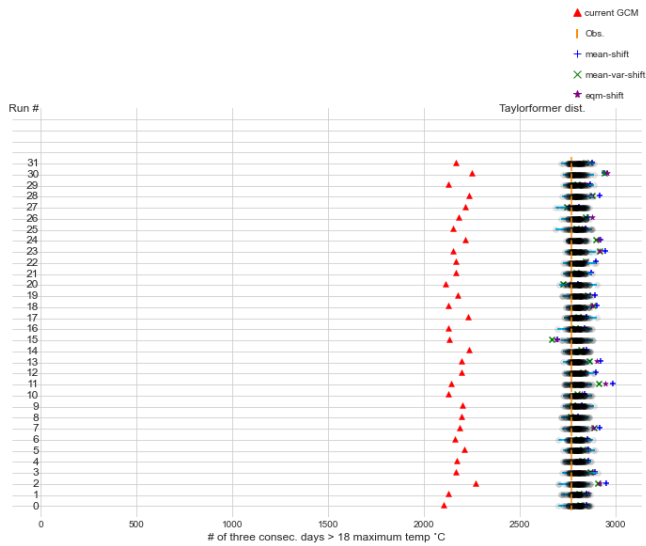
**C.2. Abuja, Nigeria**

Figure 11 shows the results for Abuja, Nigeria using a heatwave threshold of three consecutive days above 26°C maximum temperature. The raw outputs from the IPSL climate model (red triangles) underestimate the number of instances of observed heatwaves (vertical orange line) for the period 1989 – 2008. Our novel Taylorformer temporal BC produces a much more accurate distribution (horizontal box-plots) per run (0-31) for the number of heatwaves in the same period with an ensemble average differing by at most 6% from the observed number of heatwaves. Other BC models perform worse: 12%, 21%, 28% for mean-shift ('+'), mean and variance shift ('X'), and EQM ('★'), respectively.

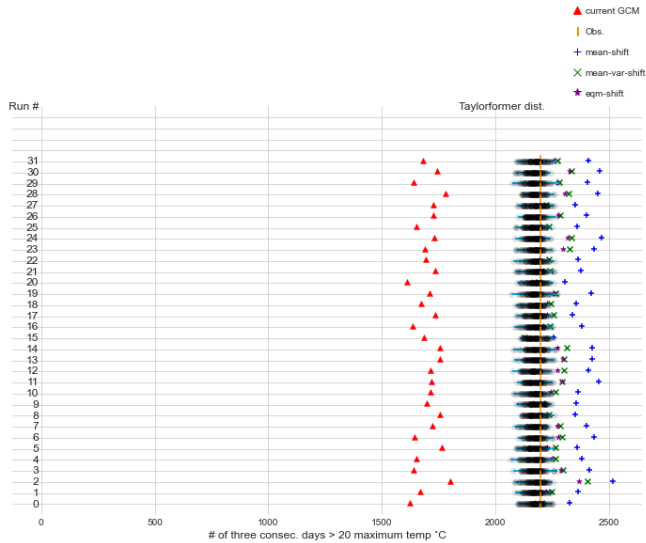
Figure 12 shows the results for Abuja, Nigeria using a heatwave threshold of three consecutive days above 28°C maximum temperature. The raw outputs from the IPSL climate model (red triangles) underestimate the number of instances of observed heatwaves (vertical orange line) for the period 1989 – 2008. Our novel Taylorformer temporal BC produces a much more accurate distribution (horizontal box-plots) per run (0-31) for the number of heatwaves in the same period with an ensemble average differing by at most 12% from the observed number of heatwaves. Other BC models perform worse: 17%, 25%, 32% for mean-shift ('+'), mean and variance shift ('X'), and EQM ('★'), respectively.

Figure 13 shows the results for Abuja, Nigeria using a heatwave threshold of three consecutive days above 30°C maximum temperature. The raw outputs from the IPSL climate model (red triangles) underestimate the number of instances of observed heatwaves (vertical orange line) for the period 1989 – 2008. Our novel Taylorformer temporal BC produces a much more accurate distribution (horizontal box-plots) per run (0-31) for the number of heatwaves in the same period with an ensemble average differing by at most 26% from the observed number of heatwaves. Other BC models perform worse: 41%, 31%, 33% for mean-shift ('+'), mean and variance shift ('X'), and EQM ('★'), respectively.

**D. Supplementary figures**



**Figure 5.** Number of periods of three consecutive days above 18°C maximum temperature in Tokyo, Japan for the period 1989 – 2008. IPSL climate model (red triangles), observations (vertical orange line), Taylorformer temporal BC (horizontal box-plots), mean-shift ('+'), mean and variance shift ('X'), and EQM ('\*').



**Figure 6.** Number of periods of three consecutive days above 20°C maximum temperature in Tokyo, Japan for the period 1989 – 2008. IPSL climate model (red triangles), observations (vertical orange line), Taylorformer temporal BC (horizontal box-plots), mean-shift ('+'), mean and variance shift ('X'), and EQM ('\*').

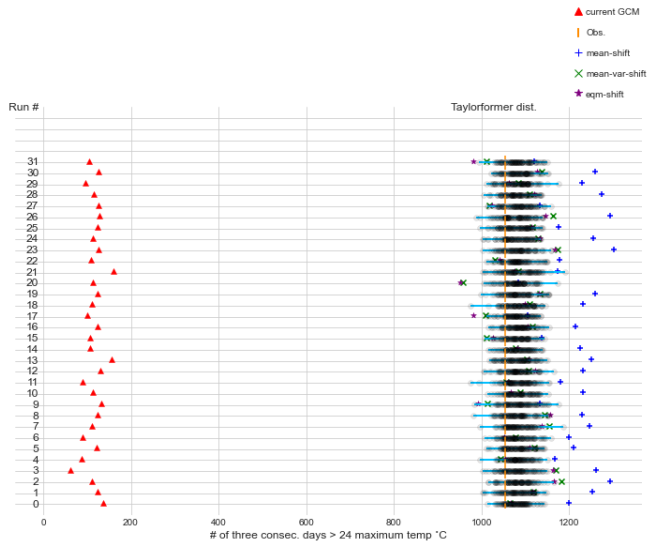


**Figure 7.** Number of periods of three consecutive days above  $24^{\circ}\text{C}$  maximum temperature in Tokyo, Japan for the period 1989 – 2008. IPSL climate model (red triangles), observations (vertical orange line), Taylorformer temporal BC (horizontal box-plots), mean-shift ('+'), mean and variance shift ('X'), and EQM ('\*').

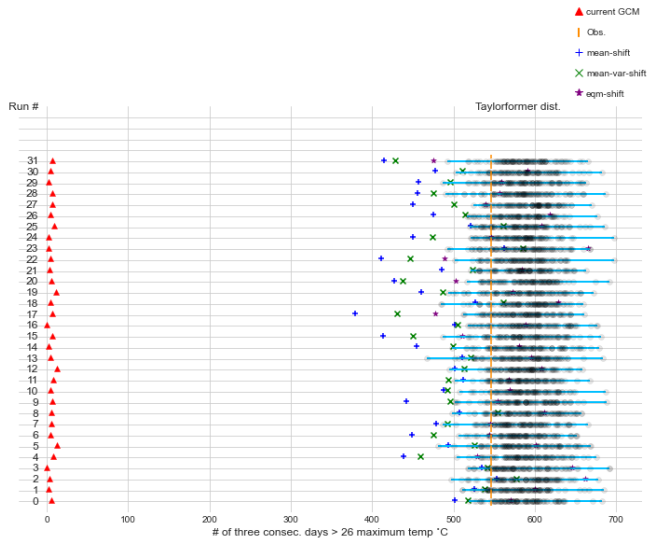


**Figure 8.** Number of periods of three consecutive days above  $26^{\circ}\text{C}$  maximum temperature in Tokyo, Japan for the period 1989 – 2008. IPSL climate model (red triangles), observations (vertical orange line), Taylorformer temporal BC (horizontal box-plots), mean-shift ('+'), mean and variance shift ('X'), and EQM ('\*').



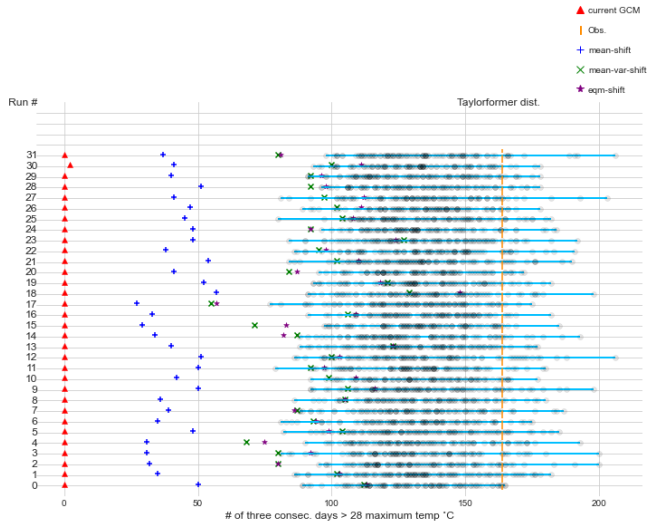


**Figure 9.** Number of periods of three consecutive days above 28°C maximum temperature in Tokyo, Japan for the period 1989 – 2008. IPSL climate model (red triangles), observations (vertical orange line), Taylorformer temporal BC (horizontal box-plots), mean-shift ('+'), mean and variance shift ('X'), and EQM ('\*').

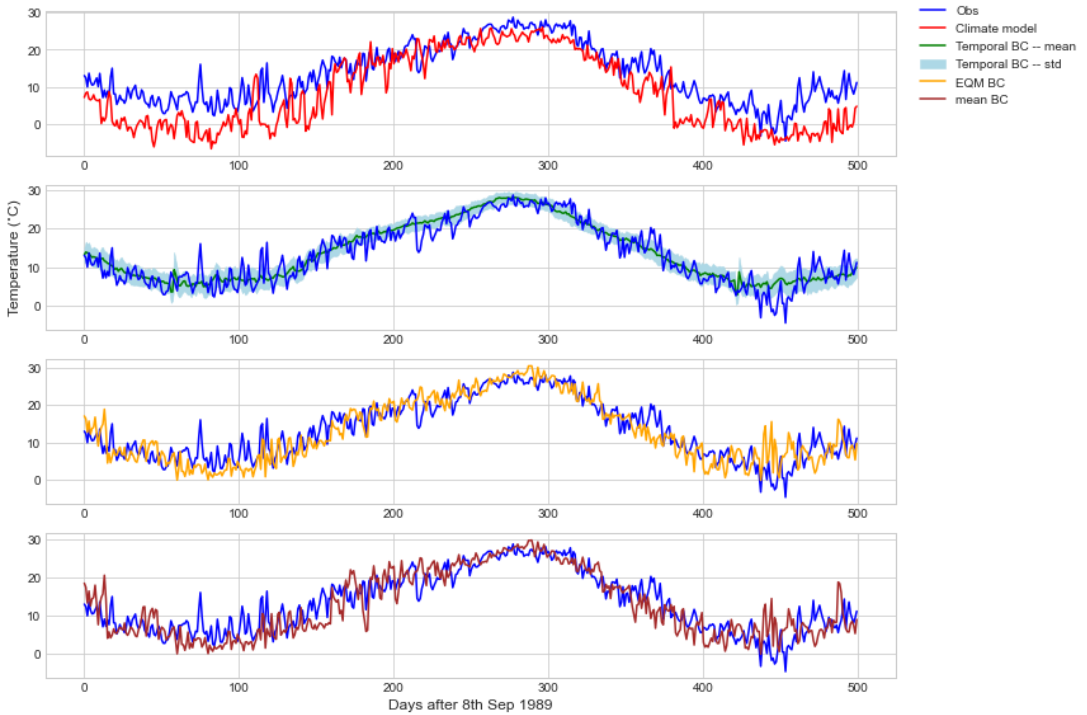


**Figure 10.** Examples for the time series trajectory output of the different BC models for 500 days after September 8-th 1989 in Tokyo, Japan. First panel: observation (blue) versus the IPSL climate model, Second panel: observations (blue) versus our temporal BC ensemble average (green) and its standard deviation (light-blue highlight), Third panel: observations versus EQM (orange), Fourth panel: observations vs mean-shift (brown).

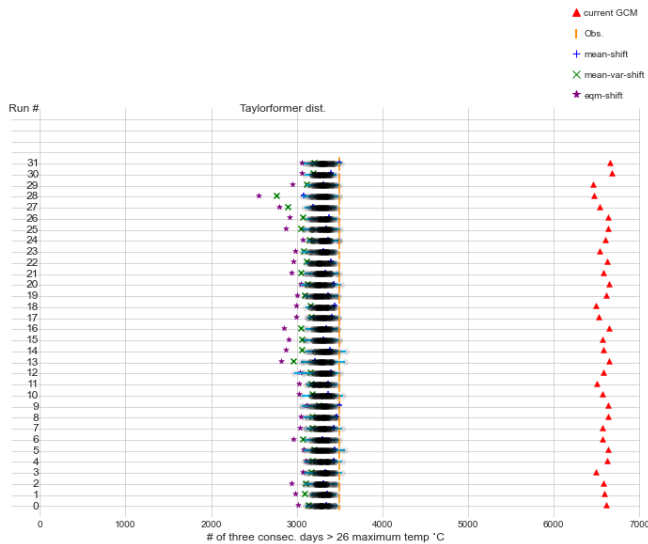


**Figure 11.** Number of periods of three consecutive days above  $26^{\circ}\text{C}$  maximum temperature in Abuja, Nigeria for the period 1989 – 2008. IPSL climate model (red triangles), observations (vertical orange line), Taylorformer temporal BC (horizontal box-plots), mean-shift ('+'), mean and variance shift ('X'), and EQM ('\*').

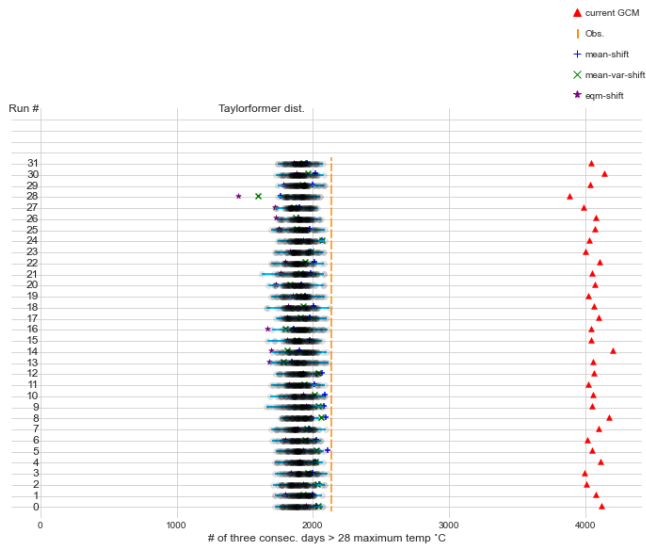


**Figure 12.** Number of periods of three consecutive days above  $28^{\circ}\text{C}$  maximum temperature in Abuja, Nigeria for the period 1989 – 2008. IPSL climate model (red triangles), observations (vertical orange line), Taylorformer temporal BC (horizontal box-plots), mean-shift ('+'), mean and variance shift ('X'), and EQM ('\*').

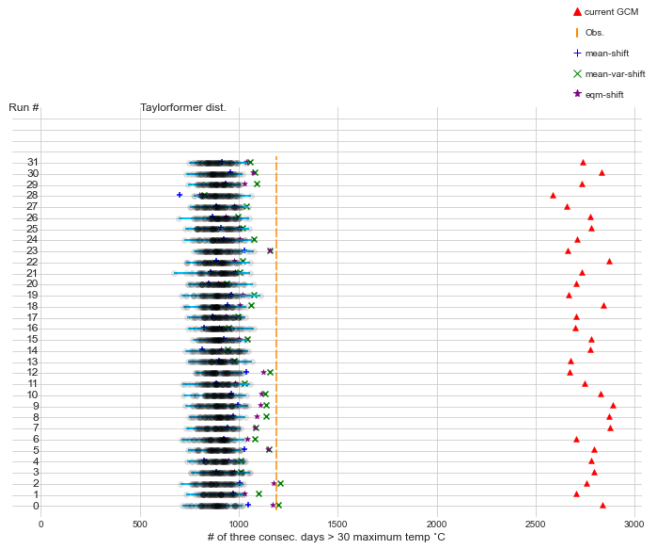


**Figure 13.** Number of periods of three consecutive days above 30°C maximum temperature in Abuja, Nigeria for the period 1989 – 2008. IPSL climate model (red triangles), observations (vertical orange line), Taylorformer temporal BC (horizontal box-plots), mean-shift ('+'), mean and variance shift ('X'), and EQM ('\*').

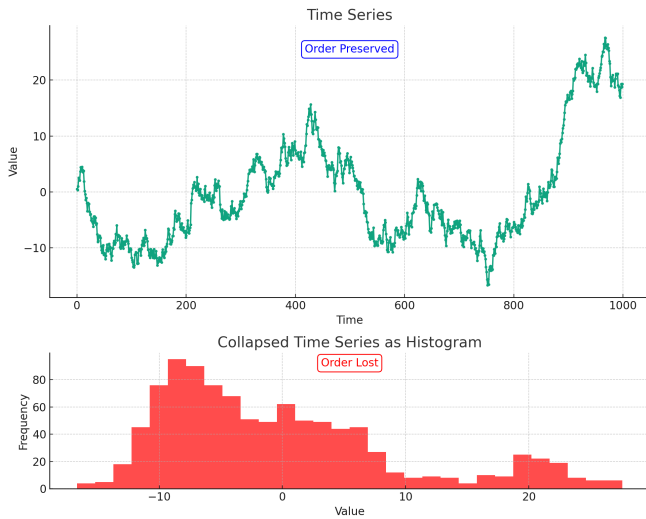


**Figure 14.** When collapsing a time-series (top) to a histogram (bottom), the temporal information is lost – a toy illustration.

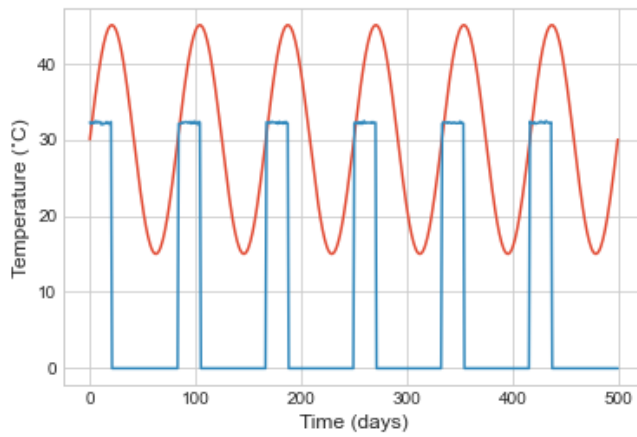


**Figure 15.** An example generated from a probability model in which 'observations' (blue line) show consistently heatwave durations that are half than those shown in 'climate model' outputs (red line).